

Cooling of Hybrid Stars with a 2SC+ $\langle dd \rangle$ Phase

Tsuneo Noda^{†1}, Akira Dohi^{‡2}, Nobutoshi Yasutake^{3,4}, Huan Chen⁵, Toshiki Maruyama⁴, and Toshitaka Tatsumi⁶

¹*Kurume Institute of Technology, Fukuoka 830-0052, Japan*

²*Interdisciplinary Theoretical and Mathematical Sciences (iTHEMS), RIKEN, Wako 351-0198, Japan*

³*Physics Department, Chiba Institute of Technology, Chiba 275-0023, Japan*

⁴*Advanced Science Research Center, Japan Atomic Energy Agency, Tokai, Ibaraki 319-1195, Japan*

⁵*School of Mathematics and Physics, China University of Geosciences, Lumo Road 388, 430074 Wuhan, China*

⁶*Kitashirakawa-Kamiikeda-Cho, Kyoto 606-8287, Japan*

.....
Recently, Fujimoto, Fukushima, & Weise (2019) have proposed a new colour-superconductive state, 2SC+ $\langle dd \rangle$ phase, which can be smoothly connected to the low-density baryon superfluidity in contrast to the 2SC phase. In this scenario, the neutron 3P_2 superfluidity on the low-density side of the phase transition is inherited by unpaired d -quarks in the 2SC phase on the high-density side. Since this could be realized in hybrid stars (neutron stars containing hadronic and quark matter), the 2SC+ $\langle dd \rangle$ phase may change the properties of neutron stars compared to the traditional 2SC phase. In this work, we study the thermal evolution of hybrid stars with the 2SC+ $\langle dd \rangle$ phase for the first time. We find that NSs with the 2SC+ $\langle dd \rangle$ phase become hotter than those with the 2SC phase, and are close to the CFL phase. The 3P_2 superfluidity plays an important role in cooling curves with not the 2SC but 2SC+ $\langle dd \rangle$ phases due to the suppression of quark β decay. We therefore point out that, if the scenario of 2SC+ $\langle dd \rangle$ phase is true, it could be specified through low-temperature observations such as Vela, 3C58, Vela Jr., and Vela-like pulsar.
.....

Subject Index D41,E32

1. Introduction

The densest star in the universe, neutron star (NS), has supra nuclear saturation density $\rho_{\text{nuc}} \simeq 2.8 \times 10^{14} \text{ g cm}^{-3}$ in their centres. In such extremely high-density matter, all baryons such as neutrons, protons, and hyperons will eventually melt and change into unbound quarks and gluons. The behavior of such a quark-hadron phase transition is still uncertain but in ultra high-density regions, deconfined quarks and gluons will compose matter since the quark-quark interactions become very weak due to the asymptotic freedom. Quark-hadron phase transition must therefore occur in the *intermediate*-density regions, where the NS

[†]noda@kurume-it.ac.jp

[‡]akira.dohi@riken.jp

core is realized. Therefore, elucidating the state of quark matter and hadron matter in the *intermediate*-density region has been a challenge in understanding the structure of neutron star cores.

In quark matter, the colour superconductive (CSC) phase appears in cold NSs (e.g, Ref. [1]). Roughly speaking, there are mainly two kinds of CSCs. One is the colour flavour-locked (CFL) phase, where all deconfined quarks are paired, while the other is the 2-flavour colour superconducting (2SC) phase, where only all strange quarks and all quarks with a colour (blue is usually chosen [2, 3]) are ungapped [4]. Because the CFL phase is the ground state in the quark matter when quark chemical potential is large enough to exceed masses of all quarks (especially strange quark), it is likely to appear in very high-density regions according to the perturbation QCD method [5, 6]. Compared with the CFL phase, the 2SC phase may occur in lower-density regions¹ [2, 9, 10].

In hadronic matter, neutron superfluidity in the 3P_2 state (and proton superconductivity in the 1S_0 state) are believed to develop over saturation density. The most promising reason for realising 3P_2 superfluidity is the measurement of nucleon-nucleon scattering phase shifts [11, 12]. It is shown that the phase shift is higher in the 3P_2 superfluidity than 1S_0 , implying strong neutrons 3P_2 pairing in the hadronic core, although its density dependence is still uncertain. Regarding protons, the 1S_0 superconductivity is likely to appear owing to their small fraction at most $\lesssim 20\%$, which effectively lowers bulk density [13, 14]. Thus, to reveal the quark-hadron phase transition, the continuity between neutrons 3P_2 pairing and ud quarks 2SC pairing should be important².

Although the conventional picture of quark-hadron phase transition is the first-order phase transition between hadronic and quark matter in the pure 2SC phase, they would not be smoothly connected because the chiral symmetry is broken in the former, but restored in the latter. As the solution, Fujimoto, Fukushima, & Weise [15] pointed out that 3P_2 neutrons superfluidity may be transformed to the 3P_2 d -quark one, which coexists with paired ud quarks (so called a 2SC+ $\langle dd \rangle$ phase), from symmetry consideration. That is, chiral symmetry and baryon number conservation are permitted to break spontaneously and simultaneously near the hadron-quark transition density, resulting in the emergence of the quark CSC phase and the baryon superfluid phase respectively. As a result, the $\langle dd \rangle$ condensate could be a key for quark-hadron continuity since it can smoothly connect with the baryon superfluid phase as well as the quark CSC phase due to common symmetry.

Physics of ultrahigh dense matter can be proven by the observation of NSs. There are mainly two approaches for this purpose. One is the overall structure of NSs, i.e., the M – R relation. The observation of masses of NSs is the strong constraint on the equation of state (EOS), such as the observations of $2M_\odot$ NSs [16–19]. The radii observations are also important such as the recent gravitational wave observations and X-ray telescope observations (e.g., for reviews of observational constraints, see Refs. [20, 21]). Using the approach with

¹ The possibility of 2SC in compact stars is still under discussion. Some studies (cf. [7]) indicate that the 2SC phase is energetically unfavourable in compact stars, but the others (cf. [8]) show that the 2SC phase can appear in compact stars with a strong coupling.

² The continuity between neutrons 3P_2 pairing and CFL pairing could also be considered, but because of large strange quark mass, $SU(3)$ flavour symmetry is broken in the density regions where quark chemical potential is not dominant. As a consequence, ud quarks pairing is natural to be considered in the intermediate density.

M – R relation, the *bulk* properties of NS matter are restricted. The other is to determine the state of high-dense matter. For this purpose, isolated NSs are one of the good observational targets to fix the cooling curves (for reviews, see Refs. [20, 22–24]). There are important observations that play the role of constraint on NS matter; Cassiopeia A observation illuminates the importance of 3P_2 superfluidity [25, 26]. ; 3C58 and Vela highlight the requirement of a strong neutrino emission process with mild suppression by superfluidity.

Considering the quark-hadron phase transition, there are pairing effects on the cooling process to satisfy the cooling observations. Too strong neutrino emission such as quark β -decay or hadronic direct Urca (DU), should be moderately suppressed by adjusting the gap. This is possible in hadronic matter due to the appearance of 3P_2 superfluidity of neutrons, but not possible in the case of the 2SC phase in quark matter. The impact of such CSC phases on cooling curves has been well examined [27–32]. In particular, Grigorian et al. (2005) [30] calculated cooling curves of hybrid stars with the 2SC phase and an additional species “X”, named as 2SC+X phase, where the density-dependent gap Δ_X is introduced as an ansatz³. They showed that the compatible gap energy of the “X” phase with the cooling data is $\Delta_X \sim 30$ keV, which is surprisingly similar to the typical 3P_2 neutrons superfluid gap $\Delta_{nn} \sim \mathcal{O}(0.01 - 0.1)$ MeV (for a review, see Refs. [12, 34]), as pointed by Ref. [35]. In that sense, the scenario of 2SC+ $\langle dd \rangle$ seems observationally favorable [36]. Considering 2SC+ $\langle dd \rangle$ phase, it is not necessary to consider the free parameter about the “X” which comes from completely mysterious origin. Also, in the 2SC+X scenario, 3P_2 and “X” coexist and it does not match with the context of Ref. [35]. In this work, we investigate the thermal evolution of hybrid stars in treating the 3P_2 states associated with both neutrons and $\langle dd \rangle$ quark without introducing the hypothetical X phase. In particular, we mostly focus on the critical temperature of 3P_2 superfluidity, which is highly uncertain (e.g., Ref. [33]).

This paper is organized as follows: In Section 2, we present the EOS adopted in this study. After introducing features of our EOS, our treatment of the neutrino cooling processes, baryon superfluidity, and quark CSC are explained, as well as the setup of our cooling calculation. Section 3 shows cooling curves and temperature structure with the 2SC+ $\langle dd \rangle$ phase, and investigates the dependence of 3P_2 superfluidity critical temperature. Section 4 devotes the conclusion.

2. Cooling Models

A. EOS

We construct the hybrid EOS with the first-order phase transition, based on the method described in Ref. [37]: In the hadronic phase, the Brueckner-Hartree-Fock method is utilized with the use of realistic two-body nucleon-nucleon potential (Bonn-B (BOB) potential [38]) and phenomenological three-body potential (Urbana UIX [39]). To investigate the concept of quark-hadron continuity, a crossover equation of state (EOS) is required in principle. However, it is difficult to determine the particle number fractions in the crossover region, as well as physical quantities such as neutrino emissivity, which are essential for cooling calculations. These values can be determined using a first-order phase transition equation

³ Grigorian et al. (2005) [30] assumes the density dependence of neutrons superfluidity (SF) in the 3P_2 state [33]. Hence, the X phase in their case would be apart from 3P_2 superfluidity.

of state. For simplicity, we calculate stellar structure using a first-order phase transition equation of state and assume that quark-hadron continuity holds under the particle fractions determined by the first-order phase transition model.

Neutrons and protons with their masses of $m_n = m_p = 939$ MeV are contained, but the degree of hyperons is not considered. Due to the uncertainties of hyperon interactions (see Ref. [40] for a review), the hyperons may play a role in the EOS. In the case of hybrid matter, however, the effects of hyperon may be relatively small because the onset density of Λ hyperons may be generally similar (or a little lower) to that of the quark phase in case of first-order phase transition [41–44]. Thus, the qualitative effects to soften the EOS can be similarly treated for both hyperons matter and quark matter. Regarding the rapid ν cooling processes, hyperon Urca processes [45] must work in particular for Λ -induced Urca [46, 47] but their dominant density regions would be very narrow due to the presence of quark β decay. Thus, the absence of a degree of hyperons could be well justified in our EOS.

In the quark phase, we employ the Dyson-Schwinger approach following Ref. [48]; To obtain the quark number density, which gives the all information of the EOS, we need to obtain the quark propagator $S(p; \mu)$ with momentum p at finite quark chemical potential μ , that is, solve the QCD's Dyson-Schwinger equation [49]⁴.

$$S^{-1}(p, \mu) = Z_2 [i\not{p} - \gamma_4 \mu + m_q] + \Sigma(p; \mu) , \quad (1)$$

where m_q is the current quark mass, where we set $m_u = m_d = 0$ and $m_s = 115$ MeV. Σ denotes the normalized self-energy. However, it is highly uncertain since it includes the non-perturbative terms such as the gluon propagator and the quark-gluon vertex at finite μ regions. Since this formalism must be connected with the hadronic physics at $\mu = 0$, we assume following self-energy extended from that in $\mu = 0$ as

$$\Sigma(p; \mu) \approx Z_1 \int^{\Lambda_{UV}} \frac{d^4 q}{(2\pi)^4} \mathcal{G}(k^2; \mu) D_{\rho\sigma}(k) \gamma_\rho S(q; \mu) \frac{\Gamma_\sigma(q, p)}{2} , \quad (2)$$

where $k \equiv p - q$, and Λ_{UV} is the ultraviolet cut-off which we take infinity. $D_{\rho\sigma}(p - q)$ is the gluon propagator independent of Landau gauge as

$$D_{\rho\sigma}(p - q) = k^{-2} \left(\delta_{\rho\sigma} - \frac{k_\rho k_\sigma}{k^2} \right) , \quad (3)$$

$\Gamma_\sigma(q, p)$ is a quark-gluon vertex at zero chemical potential. We take a widely used rainbow approximation as

$$\Gamma_\sigma(q, p) = \gamma_\sigma , \quad (4)$$

and \mathcal{G} is a effective quark-quark interaction, which we choose a Gaussian-type effective interaction as [50]

$$\mathcal{G}(k^2; \mu) = \frac{4\pi D^2}{\omega^6} k^2 \exp \left[-\frac{(k^2 + \alpha\mu^2)}{\omega^2} \right] , \quad (5)$$

⁴ We use the standard notation and conventions of Minkowski space formulation, such as $\not{A} = A_\mu \gamma^\mu = g^{\mu\nu} A_\mu \gamma_\nu$, $\{\gamma^\mu, \gamma^\nu\} = 2g^{\mu\nu}$, $\gamma_\mu^\dagger = \gamma_\mu$ and $\gamma_5 = i\gamma^0 \gamma^1 \gamma^2 \gamma^3 \gamma_4$, where $g_{00} = 1$ and $g_{\mu\mu} = -1$ for $\mu \neq 0$.

with $\omega = 0.5$ GeV, and $D = 1$ GeV². α is a parameter that controls the degree of asymptotic freedom, and we choose a typical value $\alpha = 1$ [48]. Note that this approximation reproduces a non-interacting quark matter at finite μ for $\alpha = \infty$.

Although the rainbow approximation enables us to study the self-energy Eq. (2) regardless of the remaining terms of Eq. (1)⁵, gauge covariance is lost, which leads to an unphysical solution of $S(p; \mu)$. To avoid this, we fix the renormalization constants $Z_1 = Z_2 = 1$, using Ward identity.

Once the quark propagator $S(p; \mu)$ is obtained, the number density, energy per baryon, and pressure of each quark ($q = u, d, s$) can be obtained as

$$f_q(|\mathbf{p}; \mu|) = \frac{1}{4\pi} \int_{-\infty}^{\infty} dp_4 \text{tr}_D [-\gamma_4 S(p; \mu)] \quad (6)$$

$$n_q(\mu) = 2 \cdot 3 \int \frac{d^3 p}{(2\pi)^3} f_q(|\mathbf{p}; \mu|) \quad (7)$$

$$\epsilon_q(\mu_q) = 2 \cdot 3 \int \frac{d^3 p}{(2\pi)^3} \sqrt{m_q^2 + p^2} f_q(|\mathbf{p}; \mu|) \quad (8)$$

$$P_q(\mu_q) = P_q(\mu_{q,0}) + \sum_{q=u,d,s} \int_{\mu_{q,0}}^{\mu_q} d\mu n_q(\mu) , \quad (9)$$

where the traces are applied only to spinor indices. $\mu_{q,0}$ is the theoretically arbitrary value, which we take as $\mu_{u,0} = \mu_{d,0} = 0$ and $\mu_{s,0} = 460$ MeV following Ref. [48]. $P_q(\mu_{q,0})$ is the pressure of quark matter in the vacuum, which can be regarded as the effective bag constant

$$B_{\text{DS}} = -[P_u(\mu_{u,0}) + P_d(\mu_{d,0}) + P_s(\mu_{s,0})] , \quad (10)$$

Following Ref. [48], we take $B_{\text{DS}} = 90$ MeV fm⁻³.

To obtain the EOS of NS matter, we should impose the conditions of neutrino-less beta equilibrium and charge neutrality. In hadronic-matter EOS, which contains two baryons (n, p) and electrons⁶, these are given as

$$\mu_n - \mu_p = \mu_e , \quad (11)$$

$$Y_p = Y_e \quad (12)$$

where μ_i is the chemical potential. On quark-matter EOS, which contains three-flavour (u, d, s) and electrons, these are given as

$$\mu_d = \mu_u + \mu_e , \quad (13)$$

$$\mu_d = \mu_s , \quad (14)$$

$$\frac{2Y_u - Y_d - Y_s}{3} = Y_e . \quad (15)$$

⁵ This merit arises due to the quenched approximation, which neglects fermion loop contributions to the vacuum polarisation as clearly seen in Eq. (3).

⁶ Muons are not contained in our EOS, which does not change the EOS and neutrino emissivity significantly at least in cold NSs ($T \lesssim 0.1$ MeV); The maximum mass is reduced by $\sim \mathcal{O}(0.01) M_\odot$ by including muons. Even if the muon-induced DU process ($p + \mu \rightarrow n + \nu_\mu$, $n \rightarrow p + \mu + \nu_\mu$) occurs, the electron-induced DU process has already occurred because of being more electrons than muons, and that it is stronger than muon-induced one.

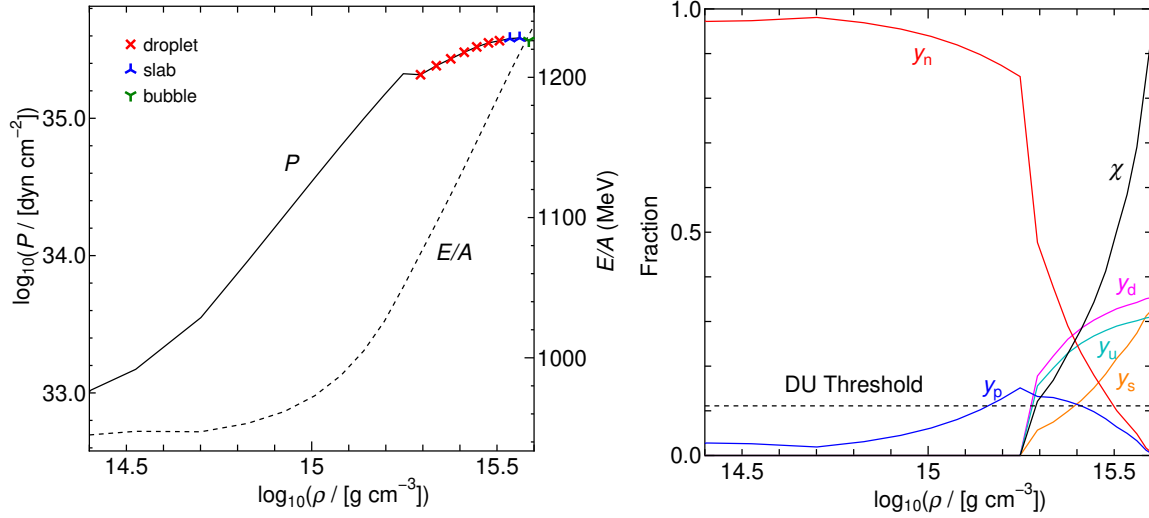


Fig. 1 Left: Energy-density dependence of pressure and energy per baryon. The inhomogeneous mixed phases are also shown as different symbols. Right: Energy-density dependence of each particle fraction and quark volume fraction χ . The critical proton fraction for the appearance of the DU process is also plotted.

To construct the hybrid star EOS, we assume the first-order phase transition between the hadron and quark phases. Then, we apply the Gibbs construction, which allows the co-existence of hadron and quark phases with the pressure P^M . Such a mixed phase is realized when the following thermodynamical conditions are satisfied:

$$P^M \equiv P^H = P^Q, \quad (16)$$

$$\mu_e^H = \mu_e^Q, \quad (17)$$

where H and Q denote hadronic and quark phases, respectively. In addition to Eqs. (11) and (13), and (14), the following conditions of beta equilibrium, i.e., the equality of baryonic chemical potential between hadron and quark phases, should be satisfied in mixed-phase:

$$\mu_n = \mu_u + 2\mu_d, \quad (18)$$

$$\mu_p = 2\mu_u + \mu_d, \quad (19)$$

Against the only six equations to describe beta equilibrium, there are seven variables, i.e., $Y_n, Y_p, Y_e, Y_u, Y_d, Y_s$, and χ . A last equation to close the system derives from the global charge neutrality as

$$(1 - \chi) Y_p + \frac{\chi}{3} (2Y_u - Y_d - Y_s) = Y_e \quad (20)$$

where $\chi \in [0, 1]$ is the volume fraction of quark matter.

To include the finite-size effects such as the Coulomb interaction and the surface tension, we employ the Wigner-Seitz approximation in the same manner as in Ref. [51] with the surface tension parameter $\sigma = 40 \text{ MeV fm}^{-2}$ (see also our review [52]). Namely, the whole space is sharply divided into the mixed-phase equivalent cells with given geometrical symmetry, which is characterized by the dimensionality d ; $d = 1, 2, 3$ corresponds to the droplet (or

bubble), rod (or tube), and slab, respectively. Thus, the volume fraction is defined as

$$\chi = \left(\frac{r_d}{r_{WS}} \right)^d, \quad (21)$$

where r_{WS} and r_d denote the size of the Wigner-Seitz cell and each geometric structure. These properties are reflected in the total internal energy, which is given in the Thomas-Fermi approximation ⁷. The volume fraction χ and the corresponding inhomogeneous mixed phase are shown in the left panel of FIG. 1. As the density increases, we can see the transition from droplet, slab, and bubble phases. We note that our EOS does not realize the uniform quark phase even with the maximum mass.

In the end, we can obtain each particle fraction as a function of baryon density ρ_B^M or energy density ρ^M in mixed-phase, which can be obtained from

$$\rho_B^M = (1 - \chi) \rho_B^H + \chi \rho_B^Q, \quad (22)$$

$$\rho^M = (1 - \chi) \rho^H + \chi \rho^Q. \quad (23)$$

Information of our EOS is summarized in FIG. 1, such as the energy density, pressure, and fraction of each particle in β -equilibrium cold matter. Our models show the first-order phase transition beyond $\rho_t \simeq 1.77 \times 10^{15} \text{ g cm}^{-3}$. In our EOS, the DU process is allowed to occur beyond $\rho_{DU} = 1.46 \times 10^{15} \text{ g cm}^{-3}$.

Once the EOS is constructed, one can obtain the mass-radius relation through the TOV equation [56, 57], which is shown in FIG. 2. As reported in Ref. [37], our hybrid EOS can account for the observations of massive $2 M_\odot$. The radius around the canonical mass $1.4 M_\odot$ is 13 km, which is consistent with many observational constraints such as GW 170817 and NICER observation of PSR J0740+6620.

B. Neutrino Emission Processes and SF/CSC

In the hadronic phase, we consider the *conventional* cooling processes (see Ref. [58] for their list), which are the same as our previous work [59, 60]: Slow neutrino cooling processes mainly composed of modified Urca, and bremsstrahlung, are always open to occur in any NSs. These emissivities are approximately

$$\epsilon_\nu^{\text{Slow}} \approx 10^{19-21} T_9^8 \text{ erg cm}^{-3} \text{ s}^{-1}, \quad (24)$$

where T_9 is the local temperature in a unit of 10^9 K .

In addition to slow cooling processes, when the temperature becomes lower than the superfluid transition temperature T_c , the pair breaking and formation (PBF) process occurs as the release of thermal energy. The emissivity is given as [61, 62]:

$$\epsilon_\nu^{\text{PBF}} \approx 10^{21-22} T_9^7 \tilde{F}_i(T/T_{\text{cr}}) \text{ erg cm}^{-3} \text{ s}^{-1}, \quad (25)$$

where $\tilde{F}_i(T/T_{\text{cr}})$ indicates the efficiency of PBF processes as a function of T/T_{cr} with 1S_0 for $i = s$ and 3P_2 baryons for $i = t$. The concrete formula of the *control function* is given as [63]:

$$\tilde{F}_i = \frac{1}{4\pi} \int d\Omega y^2 \int_0^\infty dx \frac{z^4}{1 + e^z}, \quad (26)$$

⁷Due to the finite-size effects, the charge neutrality, baryon density, and energy density, i.e., Eqs. (20), (22), and (23), respectively, are slightly modified (for the explicit formulae, see e.g., Ref. [53]), but we pay special attention to the CSC, not the description of finite-size effects in our paper, although they are fully taken into account for our EOS.

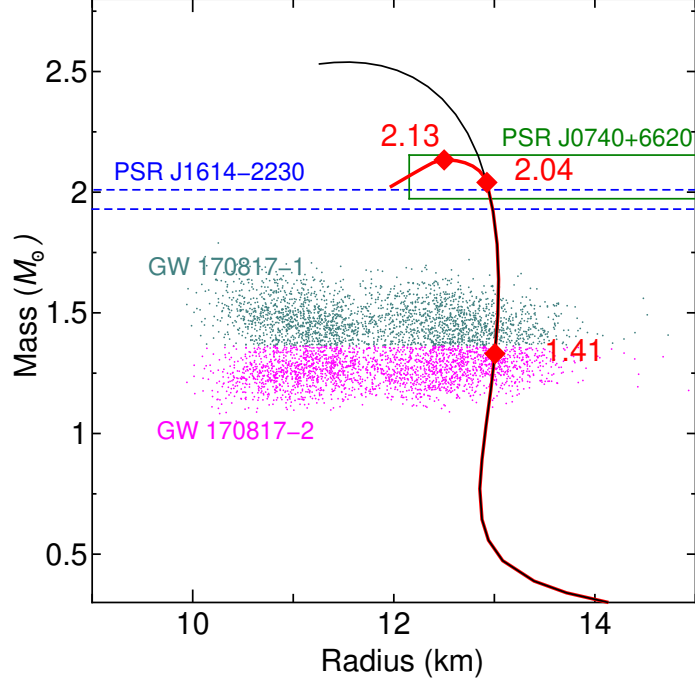
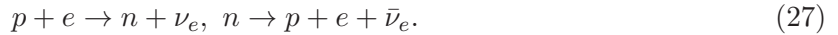


Fig. 2 Mass-radius relation in our hadronic EOS (black) and hybrid EOS (green). The chosen masses for our cooling calculation are marked as a diamond symbol. We also plot the constraints from the measured tidal deformability of two NSs before they coalesce each other (GW 170817) [54], and observed two massive pulsars J1614–2230 [16] and J0740+6620 [55].

with $z = \sqrt{x^2 + y^2}$, $y = k_i \frac{T}{T_c}$, where k_i is the conversion constant factor with the state i , and $\int d\Omega$ denotes the angle averaging integration. \tilde{F}_i has a maximum value (unity) for $T \sim 0.65(0.5)$ for ${}^3P_2({}^1S_0)$ state, respectively, and zero for $T \lesssim 0.2T_{\text{cr}}$. As we see the coefficients of Eqs. (24) and (25), the PBF process is generally stronger than slow cooling processes except for cold NSs.

We also consider the nucleon DU process, i.e., neutrino emissions through β decay and inverse- β decay:



The DU process usually occurs in heavy NSs, and the emissivity is given as

$$\epsilon_{\nu}^{\text{DU}} = 4.0 \times 10^{27} \left(\frac{m_N^*}{m_N} \right)^2 \left(\frac{\rho}{\rho_{\text{nuc}}} \right)^{2/3} T_9^6 \text{ erg cm}^{-3} \text{ s}^{-1}, \quad (28)$$

where m_N^*/m_N is the effective mass ratio of nucleons, assuming equal masses of neutrons and protons. Compared with the standard cooling processes, the DU process is strong as we see the coefficient in Eq. (27), since all observed NSs are cold enough to satisfy $T_9 \lesssim 1$ (but maybe except for the NS 1987A [64, 65]). However, the DU process is realised under conditions, where the proton fraction Y_p exceeds 1/9 with no muons present, because the momentum conservation between neutrons, protons, and electrons is satisfied. In our EOS, this corresponds to $M_{\text{DU}} \geq 1.70M_{\odot}$, where M_{DU} is the threshold of the mass where the DU process operates.

In the quark phase, we assume 2-flavour case for neutrino emissivity⁸. The dominant cooling process in unpaired quark matter is the quark β decay of

$$u + e \rightarrow d + \nu_e, \quad d \rightarrow u + e + \bar{\nu}_e. \quad (29)$$

The emissivity in the case of massless non-interacting up and down quarks is given by [66, 67]:

$$\epsilon_\nu^{\text{q}\beta\text{d}} \simeq 8.8 \times 10^{26} \alpha_s (\rho/\rho_{\text{nuc}}) Y_e^{1/3} T_9^6 \text{ erg cm}^{-3} \text{ s}^{-1}, \quad (30)$$

where α_s is the strong coupling constant and is fixed to be 0.1. This emissivity is similar to that of the DU process, and enough to cool NSs rapidly.

If quarks are paired, since most of them cannot contribute to the quark β decay, the emissivity is reduced as a function of $\exp(-T_{\text{cr},q}/T)$ (e.g., [29]), where $T_{\text{cr},q}$ is the critical temperature of CSC and assumed to be 10 MeV. In the 2SC phase, the emissivity is almost the same as Eq. (30) multiplied by 1/3. In the CFL phase, on the other hand, the quark β decay is highly suppressed and practically invalid. This can be applied to quark-modified Urca and quark bremsstrahlung processes, which are negligible in all cases because we consider cold NSs ($T_9 \lesssim 1$) and the suppression factor is quite small as $\exp(-2T_{\text{cr},q}/T)$. Instead, the dominant cooling process in quark CFL matter is electron-electron scattering as⁹

$$e + e \rightarrow e + e + \nu + \bar{\nu}, \quad (31)$$

whose neutrino emissivity is given as [70]:

$$\epsilon_\nu^{ee} = 2.8 \times 10^{12} (\rho/\rho_{\text{nuc}}) Y_e^{1/3} T_9^8 \text{ erg cm}^{-3} \text{ s}^{-1}. \quad (32)$$

In our EOS, baryons and electrons exist even in the maximum central density regions. Since the quark β decay is practically invalid due to CFL pairing, baryonic cooling processes are dominant for total neutrino emissivity.

The total neutrino emissivity in the quark-hadron mixed phase is the summation of individual emissivities shown above. Some processes have conditions and some are affected by the superfluidity or the superconductivity. Considering the quark colour superconductivity and nucleon superfluidity, and dropping significant small terms, the total neutrino emissivity can be written as

$$\begin{aligned} \epsilon_\nu^{\text{Total}} &\simeq (1 - \chi) \epsilon_\nu^{\text{PBF}} \tilde{F}_t \\ &+ f_{\text{sf}} \left((1 - \chi) \epsilon_\nu^{\text{DU}} \Theta(\rho - \rho_{\text{DU}}) \right. \\ &\left. + \chi \frac{1}{3} \epsilon_\nu^{\text{q}\beta\text{d}} \Theta(\rho - \rho_t) \right), \end{aligned} \quad (33)$$

⁸ We assume that the effect of s -quarks is not significantly large. The s -quarks decay into u -quarks which is in superconducting state (2SC component of 2SC+ $\langle dd \rangle$ phase), and the emissivity caused by s -quarks is strongly suppressed. Also, the effect of Cabibbo suppression is significantly large compared to ud -quark β decay. To demonstrate the effect of 2SC+ $\langle dd \rangle$ phase, we assume the simplest quark model which consists of u and d quarks.

⁹ In the CFL, the scattering of gluons appearing as the Nambu-Goldstone boson could be a cooling process due to the production of neutrinos, but it is quite sensitive to temperature [68, 69], and little affects cooling curves with $T \lesssim 10$ MeV.

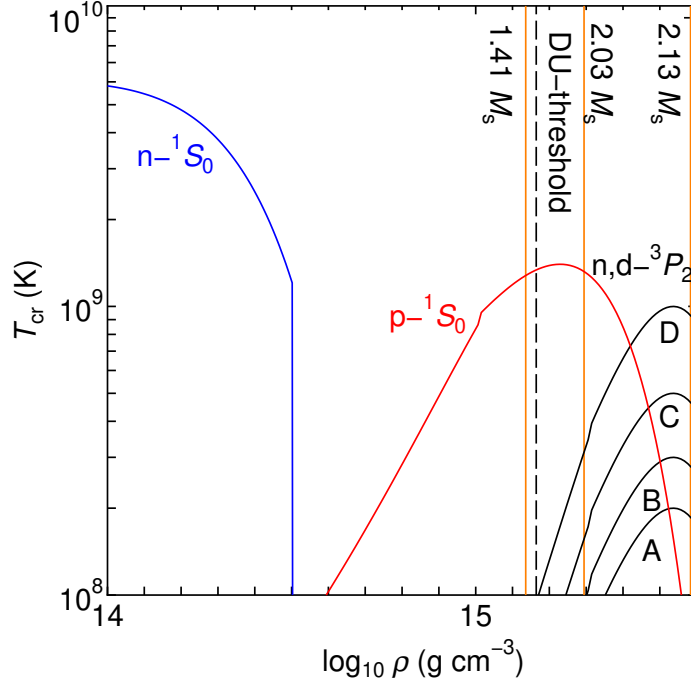


Fig. 3 Critical temperatures of each superfluid/superconductive state. Black curves show the different 3P_2 models of neutrons and unpaired d quarks. Note that the CSC state does not appear in this figure due to the high critical temperature as 10 MeV ($=1.16 \times 10^{11}$ K). Central densities corresponding to $M_{\text{NS}} = 1.41, 2.03$ and $2.13 M_{\odot}$ are drawn as orange lines. The threshold density of the DU process is also drawn as a black line.

where f_{sf} is the suppression factor by superfluidity. In very low-temperature regions compared to T_{cr} , it is given as [71]

$$f_{\text{sf}} = \exp\left(\frac{-8.4T_{\text{cr}}}{T}\right). \quad (34)$$

Here, we drop some negligible terms of neutrino emissivities of slow cooling, electron scattering, and quark β decay of 2SC-paired quarks, the last of which becomes much weaker due to the large CSC critical temperature. $\tilde{F}_t(T/T_{\text{cr}})$ indicates the efficiency of PBF processes with 3P_2 neutrons as a function of T/T_{cr} , as given by Eq. (26). Θ is the Heaviside function in respect to the density. On the other hand, low-mass NSs with $M_{\text{NS}} < M_{\text{DU}}$ obey the standard cooling scenario mainly composed of Eqs. (24) and (25), which actually depend on the neutron 3P_2 SF models as well. Moreover, the strength of the PBF process also varies with neutron 3P_2 SF models.

FIG. 3 displays our SF models. We consider the four different SF models with the 3P_2 state, which controls the strength of 2SC+ $\langle dd \rangle$ as well as the neutrons superfluidity, while other states are fixed. Following Fujimoto et al. [35] (see discussion around Eq. (19) in their paper), we set the equal critical temperature of d -quark 3P_2 to that of neutron 3P_2 . Even the neutrons, where the uncertainty of superfluidity is significant (e.g., [72]), the situation is thought to be even more complex when it comes to quarks. Although model A–D is independent of nuclear theories, the maximum critical temperature of model A–D in the 3P_2 state, $(2 - 10) \times 10^8$ K is reasonable according to nuclear models (see FIG. 1 in [72]). In particular,

model C is similar to that inferred from the observed cooling rate of Cassiopeia A [25]. The critical temperature models of 3P_2 superfluid of neutrons and d -quarks have onset density around $2 - 3 \times 10^{14}$ g/cm³ close to the model of SYHHP, which is a phenomenological model for Cas A observations [26, 72]. They appear at a higher density than theoretical models of neutron 3P_2 , which is, however, highly uncertain in high-density regions.

Note that the impact of 1S_0 SF models on cooling curves is smaller than that of 3P_2 ¹⁰.

C. Other Setup for NS cooling

We utilize the same neutron-star cooling code as in our previous study [31], which simultaneously solves TOV and thermal transport equations. The latter equation is given on the mass coordinates M_r : ($c = G = 1$) [73, 74]:

$$\frac{\partial(L_r e^{2\phi})}{\partial M_r} = -e^{2\phi} \left(\varepsilon_\nu + e^{-\phi} C_V \frac{\partial T}{\partial t} \right), \quad (35)$$

$$\begin{aligned} \frac{\partial \ln T}{\partial \ln P} &= \frac{3}{16\pi} \frac{\kappa L_r P}{M_{tr} a T^4} \frac{\rho_0}{\rho} \left(1 + \frac{P}{\rho} \right)^{-1} \times \\ &\quad \left(1 + \frac{4\pi r^3 P}{M_{tr}} \right)^{-1} \left(1 - \frac{2M_{tr}}{r} \right)^{1/2} \\ &\quad + \left[1 - \left(1 + \frac{P}{\rho} \right)^{-1} \right], \end{aligned} \quad (36)$$

where M_{tr} and M_r are gravitational and rest masses enclosed in a radius r ; ρ and ρ_0 denote the total mass-energy and rest mass densities; P , T , and L_r are the pressure, local temperature, and local photon luminosity, respectively, ε_ν denotes the energy loss rate by neutrino emission; ϕ is the gravitational potential in unit mass; a is the Stefan-Boltzmann constant; C_V is the specific heat; κ is the opacity. As the boundary condition, we impose *radiative zero boundary condition* at a sufficiently closed area to the photosphere [75]. By solving Eqs. (35), (36) and the TOV equations numerically, we can obtain the time evolution of the luminosity, and the surface temperature via Stefan-Boltzmann law.

Regarding the surface compositions, we mostly consider the ${}^{56}\text{Fe}$ surface, corresponding to the absence of light elements onto the NS. However, surface compositions are one of the important ingredients in cooling curves, although they have nothing to do with the properties of interior NSs such as the CSC. For Model C, therefore, we also consider the pure ${}^4\text{He}$ surface, which roughly gives the maximum amount of light elements.

In terms of age and observational data, we mostly take the same data as in our previous work [31]. In particular, the Vela is cold for its age, and its observational data has small uncertainties compared to others. Furthermore, we also consider the observational data of PSR J0205+6449 (in supernova remnant 3C58)¹¹, PSR B2334+61 (often called Vela-like

¹⁰ It is possible that, as the density increases, the superconductive phase of protons in the 1S_0 state may move to the two ud plus uu pairs, $2\text{SC}+\langle uu \rangle$ phase. However, the impact of the $2\text{SC}+\langle uu \rangle$ phase seems very minor compared to the $2\text{SC}+\langle dd \rangle$ because of following reasons:

- The critical temperature of 1S_0 is higher typically by 1-2 orders of magnitude than 3P_2 .
- Neutrons are always more than protons as shown in FIG. 1.

¹¹ The supernova remnant 3C 58 and the CCO PSR J0205+6449 have been thought to be associated with the historical supernova SN 1181. However, recent analysis of SN 1181 indicates that another

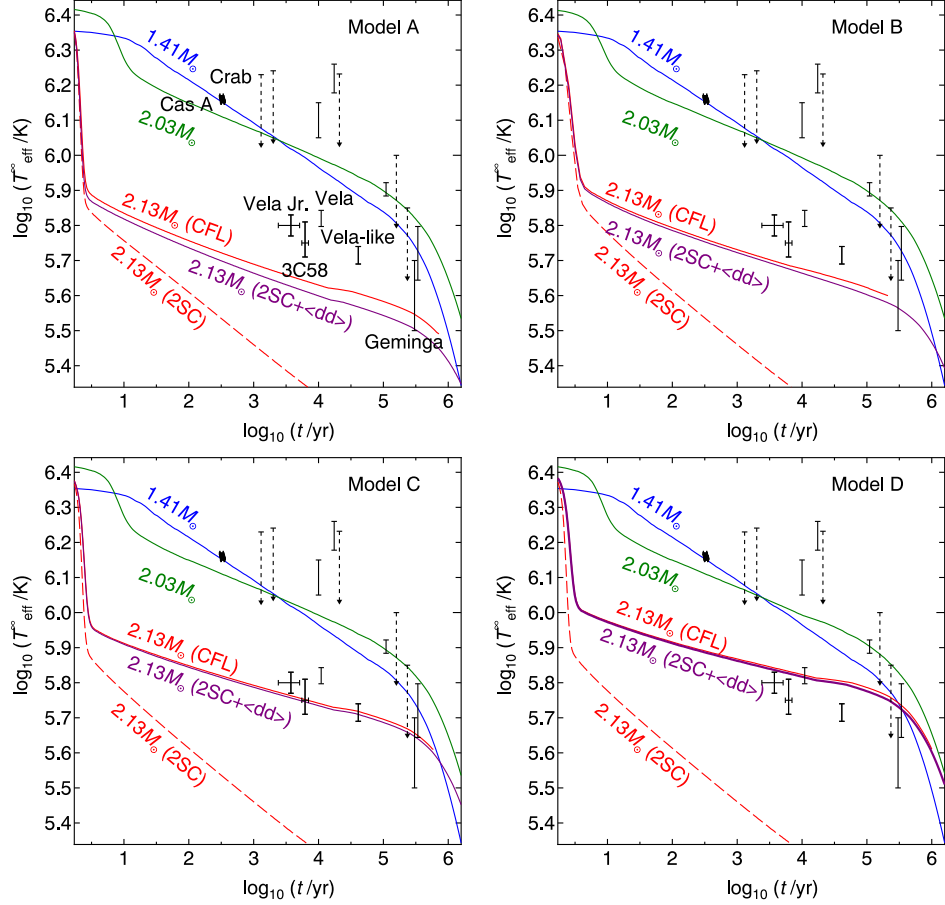


Fig. 4 Cooling curves with various superfluid models. The blue (green) line denotes $1.41M_{\odot}$ ($2.03M_{\odot}$), respectively. The red solid (dashed) line denotes $2.13M_{\odot}$ with CSC pairing of CFL (2SC), respectively. The purple line denotes $2.13M_{\odot}$ with 2SC+ $\langle dd \rangle$ model. Each superfluid model is shown on the right-top corners of each panel.

pulsar), and CXOU J0852–4617 (or Vela Jr.), which have been very recently estimated based on the analysis of XMM–Newton and Chandra data [77]¹². They identified these three cold NSs for their ages even compared to Vela, which is beyond a minimal cooling scenario¹³. Hence, these four NSs must be strong constraints to probe the compositions of high-density matter.

3. Results

FIG. 4 shows various cooling curves in our hybrid star EOS; For $2.13 M_{\odot}$ NSs, where the quark phase is allowed to appear, we show three scenarios of CSC of only 2SC phase, only

nebula Pa30 exists near the position of the supernova, and that the expansion rate of the nebula matches the 1181 event [76]. We adopt the age of 3C 58 derived from the expansion velocity of the remnant rather than from the historical event.

¹² The age of 3C58 and Vela Jr. are quite uncertain. The former derives from the significant difference between the historical record and observed expansion rate of the supernova remnant [78]. The latter is due to the lack of reliable historical records [79, 80].

¹³ This implication itself has been well known (e.g., Ref. [81]), though no lower bounds of surface temperature of the three NSs were there so far.

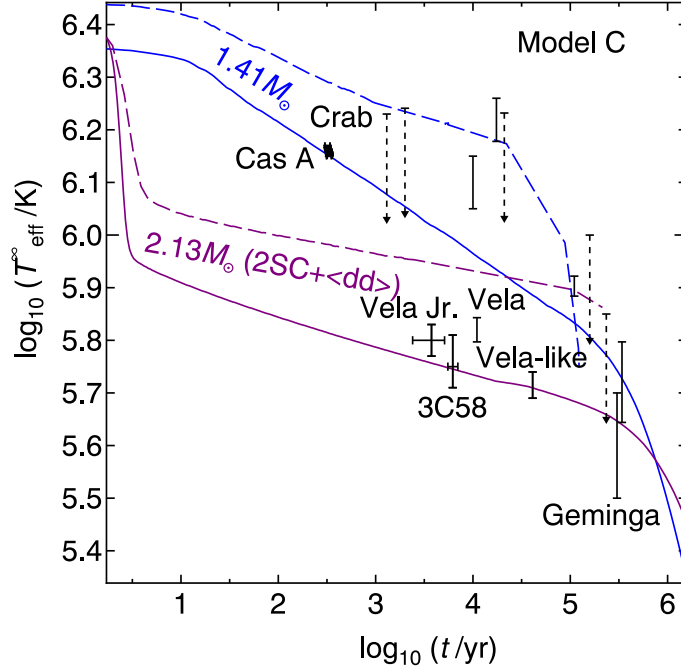


Fig. 5 Cooling curves with Model C, $M_{\text{NS}} = 1.41, 2.13 M_{\odot}$, and pure Fe envelope (solid line) and He envelope (dashed line).

CFL phase, and $2\text{SC}+\langle dd \rangle$ phase¹⁴. On the other hand, our models with 1.4 and $2 M_{\odot}$ NSs are composed of hadronic matter. These light NSs show moderate cooling behavior, as any of the fast cooling processes do not occur. In the early stage ($t < 1000$ yr), $2 M_{\odot}$ NSs cools faster than $1.4 M_{\odot}$, but it becomes opposite in the late stage. This is because the higher-mass models show higher central density, leading to higher neutrino luminosity. And, since the neutrino emissivity is sensitive to the temperature ($\propto T^{7-8}$ in these cases), neutrino luminosity decreases rapidly for higher-mass models. The mass relationship within the standard cooling scenario we show is consistent with many literature (e.g., Ref. [82]).

In cooling curves with $2.13 M_{\odot}$ NSs, the surface temperature is much lower than the standard cooling models with 1.4 and $2 M_{\odot}$ NSs. In particular, the models with the 2SC phase show supra-rapid cooling compared with CFL and $2\text{SC}+\langle dd \rangle$ phases, which show similar cooling curves. Thus, we can distinguish 2SC and $2\text{SC}+\langle dd \rangle$ from temperature observations. We also find that the 3P_2 superfluidity makes NSs warm with these models.

In model A (the maximum critical temperature with neutrons 3P_2 state of $\max(T_{cr}^{n3}) = 2 \times 10^8$ K), cooling curves are located in lower temperature regions than all temperature observations, with any kinds of CSC. In the case of Model C ($\max(T_{cr}^{n3}) = 5 \times 10^8$ K), three new observations of 3C58, Vela Jr., and Vela-like pulsar are passed through a cooling curve with CFL and $2\text{SC}+\langle dd \rangle$, not 2SC phase. Thus, the $2\text{SC}+\langle dd \rangle$ phase is observational better than the only 2SC . Although Vela is higher than all the cooling curves, it would be explained with either lower-mass NSs or lighter surface compositions, which tend to be warmer.

¹⁴ For simplicity, we consider the case where either 2SC (or $2\text{SC}+\langle dd \rangle$) or CFL is allowed, but their combination is possible because they can be smoothly connected in regard with the symmetry [35].

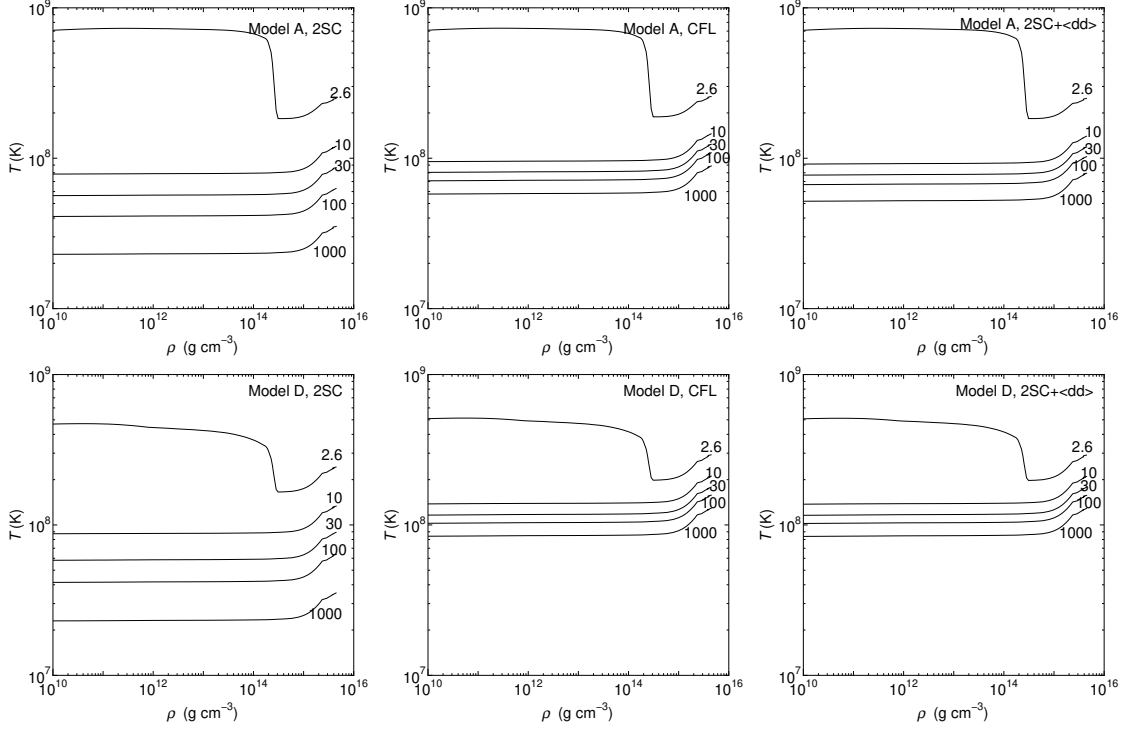


Fig. 6 Time evolution of temperature structure with SF model A (top) and D (bottom). The quark CSC is the only 2SC (left), the only CFL (middle), and 2SC+ $\langle dd \rangle$ (right). The numerals attached to the curves show the ages (yr).

Model D ($\max(T_{cr}^{n3}) = 1 \times 10^9$ K) can explain the observation data of Vera by considering the 2SC+ $\langle dd \rangle$ (or CFL) phase, but it cannot explain the lower limit of the observation with the 2SC phase. But recently updated three observations are still too cold to be explained due to the large suppression of rapid cooling processes even with 2SC+ $\langle dd \rangle$ or CFL phase. As the maximum mass with our EOS is $\approx 2.13 M_{\odot}$, we suggest that strong neutrons 3P_2 superfluidity with $\max(T_{cr}^{n3}) \gtrsim 10^9$ K is not plausible. Considering that very weak neutron superfluidity such as Model A results in too rapid cooling compared to the observations as well, the suitable one is like Model C ($\max(T_{cr}^{n3}) = 5 \times 10^8$ K) or slightly strong neutrons 3P_2 SF models. Coincidentally, this result is consistent with the constraint of $\max(T_{cr}^{n3})$ obtained from the observed cooling rates of Cassiopeia A [83].

For our best cooling model with Model C, we show the comparison of cooling curves between pure Fe and He envelope in FIG 5. If there are light elements in the NS envelope, cooling curves tend to be located in higher temperature regions because the thermal conductivity of light elements is lower than that of Fe. This can be seen in both the slow cooling case ($M_{NS} = 1.41 M_{\odot}$) and the fast cooling case ($2.13 M_{\odot}$). By changing surface compositions, the consistency with the observations is changed. For example, $2.13 M_{\odot}$ NSs with pure Fe surface compositions are colder than the observed surface temperature of Vela, but the relationship becomes the opposite for the pure He surface compositions. This implies that, if Model C is true as the 3P_2 SF model, the surface compositions of Vela are intermediate between He and Fe. Thus, the uncertainties of surface compositions could alter the appropriate 3P_2 SF model.

FIG. 6 shows the internal temperature with models A and D. Let us consider model A, where the 3P_2 SF is weakest in our models. At $t = 2.6$ yr, the NS core cools rapidly due to the presence of the DU process. Although the quark β decay is active with the 2SC and 2SC+ $\langle dd \rangle$ phase, the temperature structure is similar among different CSC states. The difference in CSC appears after the realization of isothermal structure for $t \gtrsim 10$ yr: The temperature with the 2SC phase rapidly decreases compared to the models with the 2SC+ $\langle dd \rangle$ and CFL phases. It should be mentioned that even the weakest 3P_2 SF alters the temperature structure when we compare it with the 2SC and 2SC + $\langle dd \rangle$ phases.

If the 3P_2 SF model is changed from A to D, you can see that the temperature becomes higher with the CFL and 2SC+ $\langle dd \rangle$ phases, but cannot see so much with the 2SC phase. This is because the quark β decay, which is derived from d quarks in the 3P_2 state, is suppressed except in the 2SC phase. Thus, we suggest that the 3P_2 superfluidity plays an important role in the 2SC+ $\langle dd \rangle$ scenario.

Considering CSC, there is an issue. The CFL pairing is suitable for the cooling results which show moderately strong cooling (due to the DU process), but the appearing density is thought to be much higher density. On the other hand, the 2SC pairing is suitable for the appearing density, but the cooling result shows too strong cooling to explain the observation. The 2SC+ $\langle dd \rangle$ phase can solve this problem, as already suggested by Ref. [30] in the 2SC+X scenario. The appearing density of 2SC+ $\langle dd \rangle$ is suitable for the realistic density of NS, and it *can* suppress strong neutrino emission by quarks in all colours.

4. Conclusion

We investigate the thermal evolution of hybrid stars with 2SC+ $\langle dd \rangle$ phase which is expected from a new picture of quark-hadron continuity proposed by Ref. [35]. We found that cooling curves are drastically changed between 2SC and 2SC+ $\langle dd \rangle$ phases, the latter of which is close to the CFL phase. Thus, we can clarify the difference between the 2SC and 2SC+ $\langle dd \rangle$ phases through temperature observations such as Vela.

We also found that 3P_2 superfluidity, associated with neutrons as well as d quarks, plays an important role in the thermal evolution of NS in the case of the 2SC+ $\langle dd \rangle$ as well as the CFL phase. This is a crucial difference compared to the only 2SC phase, where the 3P_2 superfluidity is not so important due to unsuppressed quark β decay. If the (maximum) 3P_2 superfluid temperature lies in $5 \times 10^8 \text{ K} \lesssim \max(T_{cr}^{n3}) < 10^9 \text{ K}$, the 2SC+ $\langle dd \rangle$ phase can account for the recent temperature observation of cold NSs such as Vela, 3C58, Vela Jr., and Vela-like pulsar, and therefore it is favored from temperature observations compared to the 2SC.

We adopted the hybrid EOS where the quark matter is constructed with the Dyson-Schwinger approach, which does not consider the di-quark condensation needed for the description of CSC. In regard to this, one of the concerns is that the mass-radius relationship may be changed. In the scenario with the 2SC+X phase, there is a kink structure to make the radius large at some masses regions. Since this can be regarded as the higher slope of the symmetry energy [84], the proton fraction around the kink regions may be increased [15] and the DU process can be allowed in lower-mass NSs. However, our EOS also allows for the DU process, and the change from cooling curves in this paper is the only threshold mass of the DU process.

However, if di-quark condensation is incorporated in the EOS of quark matter, the appearance density of $2SC+\langle dd \rangle$ must be changed. The transition between $2SC+\langle dd \rangle$ and CFL is also highly possible, though we did not consider such a case. The consistent cooling calculation with the EOS in terms of the CSC (and baryon SF) is left for future work. Although there are many assumptions about nuclear models, this work is the first cooling calculation to consider quark-hadron continuity through the *unified* 3P_2 superfluid model. Thus, we hope that this work provides the basis to pursue the evidence of another CSC state beyond the standard picture of the 2SC and CFL phases.

Recently-updated observations of cold NSs (3C58, Vela Jr., and Vela-like pulsar) beyond the minimal cooling scenario [77] offer us a strong motivation to probe the exotic states in high-density matter. Our study is the first work to explore exotic states inside NSs with these updated observations. In particular, as fast neutrino cooling must be suppressed by the pairing for their observations, even with other EOSs, we believe it common that some kinds of superfluidity inside the NS core should not be too strong, such as the 3P_2 neutron superfluidity considered here. The desired information is their masses, which are little known (though they must be heavy due to the rapid cooling). If the mass measurement is fortunately performed in the future, with such as NICER, internal states (compositions and superfluidity/superconductivity) in NSs will be well determined. As one of the ingredients, the presence or absence of $2SC+\langle dd \rangle$ examined in our work may possibly be judged.

In this study, we have assumed two major premises. One is that the EOS takes into account quark-hadron continuity by concerning first-order phase transitions; the other is that the critical temperature of the neutron's 3P_2 state is continuously linked to that of the d -quark. The former issue concerns the difficulty in defining the particle number fraction required for cooling calculations when considering the crossover EOS, whilst the latter concerns the excessive uncertainty surrounding the realistic 3P_2 critical temperature of the d -quark. We hope that in the near future we will be able to set aside these assumptions and engage in a self-consistent discussion.

We thank T. Hatsuda for an informative discussion and Y. Fujimoto for careful reading of our manuscript. We thank the referee for the constructive comments, which helped improve the manuscript. T.N. wishes to acknowledge the support from the Discretionary Budget of the President of Kurume Institute of Technology. This work is also supported by JSPS KAKENHI Grant Numbers JP23K19056, JP25K17403 (A.D.), JP24K07054, (N.Y.) and JP26K07094 (T.N.).

References

- [1] K. Fukushima, and T. Hatsuda, Reports on Progress in Physics**74**, 014001 (2011) arXiv:1005.4814.
- [2] A.W. Steiner, S. Reddy, and M. Prakash, Phys. Rev. D**66**, 094007 (2002) arXiv:hep-ph/0205201.
- [3] M.G. Alford, J.A. Bowers, J.M. Cheyne, and G.A. Cowan, Phys. Rev. D**67**, 054018 (2003) arXiv:hep-ph/0210106.
- [4] D. Bailin, and A. Love, Phys. Rep. **107**, 325–385 (1984).
- [5] M. Alford, K. Rajagopal, and F. Wilczek, Physics Letters B**422**, 247–256 (1998) arXiv:hep-ph/9711395.
- [6] M. Alford, K. Rajagopal, and F. Wilczek, Nuclear Physics B**537**, 443–458 (1999) arXiv:hep-ph/9804403.
- [7] M. Alford, and K. Rajagopal, Journal of High Energy Physics**2002**, 031 (2002) arXiv:hep-ph/0204001.
- [8] H. Abuki, and T. Kunihiro, Nucl. Phys. A**768**, 118–159 (2006) arXiv:hep-ph/0509172.
- [9] F. Neumann, M. Buballa, and M. Oertel, Nucl. Phys. A**714**, 481–501 (2003) arXiv:hep-ph/0210078.
- [10] M.G. Alford, A. Schmitt, K. Rajagopal, and T. Schäfer, Reviews of Modern Physics**80**, 1455–1515 (2008) arXiv:0709.4635.
- [11] R. Tamagaki, Progress of Theoretical Physics**44**, 905–928 (1970).

-
- [12] D. Page, J.M. Lattimer, M. Prakash, and A.W. Steiner, Eds. K. H. Bennemann and J. B. Ketterson, (2013) arXiv:1302.6626.
- [13] T. Takatsuka, and R. Tamagaki, Progress of Theoretical Physics Supplement**112**, 27–65 (1993).
- [14] J. Wambach, T.L. Ainsworth, and D. Pines, Nucl. Phys. A**555**, 128–150 (1993).
- [15] T. Kojo, D. Hou, J. Okafor, and H. Togashi, Phys. Rev. D**104**, 063036 (2021) arXiv:2012.01650.
- [16] P.B. Demorest, T. Pennucci, S.M. Ransom, M.S.E. Roberts, and J.W.T. Hessels, Nature **467**, 1081–1083 (2010) arXiv:1010.5788.
- [17] J. Antoniadis, P.C.C. Freire, N. Wex, T.M. Tauris, and R.S. Lynch *et al.*, Science**340**, 448 (2013) arXiv:1304.6875.
- [18] H.T. Cromartie, E. Fonseca, S.M. Ransom, P.B. Demorest, and Z. Arzoumanian *et al.*, Nat. Astron.**4**, 72–76 (2020) arXiv:1904.06759.
- [19] R.W. Romani, D. Kandel, A.V. Filippenko, T.G. Brink, and W. Zheng, Astrophys. J. Lett. **934**, L17 (2022) arXiv:2207.05124.
- [20] G.F. Burgio, H.J. Schulze, I. Vidaña, and J.B. Wei, Progress in Particle and Nuclear Physics**120**, 103879 (2021) arXiv:2105.03747.
- [21] B.A. Li, B.J. Cai, W.J. Xie, and N.B. Zhang, Universe**7**, 182 (2021) arXiv:2105.04629.
- [22] D.G. Yakovlev, and C.J. Pethick, Ann. Rev. Astron. Astrophys. **42**, 169–210 (2004) arXiv:astro-ph/0402143.
- [23] D. Page, U. Geppert, and F. Weber, Nucl. Phys. A**777**, 497–530 (2006) arXiv:astro-ph/0508056.
- [24] M. Kim, C.H. Lee, Y.M. Kim, K. Kwak, Y. Lim, and C.H. Hyun, International Journal of Modern Physics E**29**, 2030007 (2020).
- [25] D. Page, M. Prakash, J.M. Lattimer, and A.W. Steiner, Phys. Rev. Lett. **106**, 081101 (2011) arXiv:1011.6142.
- [26] P.S. Shternin, D.G. Yakovlev, C.O. Heinke, W.C.G. Ho, and D.J. Patnaude, Mon. Not. Roy. Astron. Soc. **412**, L108–L112 (2011) arXiv:1012.0045.
- [27] D. Page, M. Prakash, J.M. Lattimer, and A.W. Steiner, Phys. Rev. Lett. **85**, 2048–2051 (2000) arXiv:hep-ph/0005094.
- [28] D. Blaschke, T. Klähn, and D.N. Voskresensky, Astrophys. J. **533**, 406–412 (2000) arXiv:astro-ph/9908334.
- [29] D. Blaschke, H. Grigorian, and D.N. Voskresensky, Astron. Astrophys. **368**, 561–568 (2001) arXiv:astro-ph/0009120.
- [30] H. Grigorian, D. Blaschke, and D. Voskresensky, Phys. Rev. C**71**, 045801 (2005) arXiv:astro-ph/0411619.
- [31] T. Noda, M.a. Hashimoto, N. Yasutake, T. Maruyama, T. Tatsumi, and M. Fujimoto, Astrophys. J. **765**, 1 (2013) arXiv:1109.1080.
- [32] A. Sedrakian, European Physical Journal A**52**, 44 (2016) arXiv:1509.06986.
- [33] T. Takatsuka, and R. Tamagaki, Prog. Theor. Phys. **112**, 37–72 (2004) arXiv:nucl-th/0402011.
- [34] A. Sedrakian, and J.W. Clark, European Physical Journal A**55**, 167 (2019) arXiv:1802.00017.
- [35] Y. Fujimoto, K. Fukushima, and W. Weise, Phys. Rev. D**101**, 094009 (2020) arXiv:1908.09360.
- [36] T. Noda, N. Yasutake, M.a. Hashimoto, T. Maruyama, and T. Tatsumi, , Cooling of neutron stars with quark-hadron continuity, In European Physical Journal Web of Conferences volume 260 of European Physical Journal Web of Conferences page 11024 (2022).
- [37] N. Yasutake, H. Chen, T. Maruyama, and T. Tatsumi, , Finite size effects in hadron-quark phase transition by the Dyson-Schwinger method, In Journal of Physics Conference Series volume 665 of Journal of Physics Conference Series page 012068 (2016) arXiv:1309.1954.
- [38] R. Machleidt, K. Holinde, and C. Elster, Phys. Rep. **149**, 1–89 (1987).
- [39] B.S. Pudliner, V.R. Pandharipande, J. Carlson, S.C. Pieper, and R.B. Wiringa, Phys. Rev. C**56**, 1720–1750 (1997) arXiv:nucl-th/9705009.
- [40] L. Tolos, and L. Fabbietti, Progress in Particle and Nuclear Physics**112**, 103770 (2020) arXiv:2002.09223.
- [41] T. Maruyama, S. Chiba, H.J. Schulze, and T. Tatsumi, Phys. Rev. D**76**, 123015 (2007) arXiv:0708.3277.
- [42] T. Miyatsu, M.K. Cheoun, and K. Saito, Astrophys. J. **813**, 135 (2015) arXiv:1506.05552.
- [43] Z. Bai, H. Chen, and Y.x. Liu, Phys. Rev. D**97**, 023018 (2018) arXiv:1707.09535.
- [44] P. Qin, Z. Bai, S. Wang, C. Wang, and S.x. Qin, Phys. Rev. D**107**, 103009 (2023) arXiv:2301.02768.
- [45] M. Prakash, M. Prakash, J.M. Lattimer, and C.J. Pethick, Astrophys. J. Lett. **390**, L77 (1992).
- [46] T. Takatsuka, S. Nishizaki, Y. Yamamoto, and R. Tamagaki, Progress of Theoretical Physics**115**, 355–379 (2006) arXiv:nucl-th/0601043.
- [47] C.O. Heinke, P.G. Jonker, R. Wijnands, C.J. Deloye, and R.E. Taam, Astrophys. J. **691**, 1035–1041 (2009) arXiv:0810.0497.
- [48] H. Chen, M. Baldo, G.F. Burgio, and H.J. Schulze, Phys. Rev. D**84**, 105023 (2011) arXiv:1107.2497.
- [49] C.D. Roberts, and A.G. Williams, Progress in Particle and Nuclear Physics**33**, 477–575 (1994)

-
- arXiv:hep-ph/9403224.
- [50] R. Alkofer, P. Watson, and H. Weigel, *Phys. Rev. D* **65**, 094026 (2002) arXiv:hep-ph/0202053.
 - [51] N. Yasutake, T. Maruyama, and T. Tatsumi, *Phys. Rev. D* **80**, 123009 (2009) arXiv:0910.1144.
 - [52] N. Yasutake, T. Noda, H. Sotani, T. Maruyama, and T. Tatsumi, pages 63–112 (2013) arXiv:1208.0427.
 - [53] M. Mariani, and G. Lugones, arXiv e-prints page arXiv:2308.13973 (2023) arXiv:2308.13973.
 - [54] B.P. Abbott, R. Abbott, T.D. Abbott, F. Acernese, L. Ackley, , K. *et al.* and Virgo Collaboration, *Phys. Rev. Lett.* **121**, 161101 (2018) arXiv:1805.11581.
 - [55] M.C. Miller, F.K. Lamb, A.J. Dittmann, S. Bogdanov, Z. Arzumanyan, K.C. Gendreau, S. Guillot, W.C.G. Ho, J.M. Lattimer, M. Loewenstein, S.M. Morsink, P.S. Ray, M.T. Wolff, C.L. Baker, T. Cazeau, S. Manthripragada, C.B. Markwardt, T. Okajima, S. Pollard, I. Cognard, H.T. Cromartie, E. Fonseca, L. Guillemot, M. Kerr, A. Parthasarathy, T.T. Pennucci, S. Ransom, and I. Stairs, *Astrophys. J. Lett.* **918**, L28 (2021) arXiv:2105.06979.
 - [56] R.C. Tolman, *Physical Review* **55**, 364–373 (1939).
 - [57] J.R. Oppenheimer, and G.M. Volkoff, *Physical Review* **55**, 374–381 (1939).
 - [58] D.G. Yakovlev, A.D. Kaminker, O.Y. Gnedin, and P. Haensel, *Phys. Rep.* **354**, 1–155 (2001) arXiv:astro-ph/0012122.
 - [59] A. Dohi, K. Nakazato, M.a. Hashimoto, M. Yasuhide, and T. Noda, *Prog. Theor. Exp. Phys.* **2019**, 113E01 (2019) arXiv:1910.01431.
 - [60] A. Dohi, H. Liu, T. Noda, and M.A. Hashimoto, *International Journal of Modern Physics E* **31**, 2250006 (2022) arXiv:2112.13302.
 - [61] D.G. Yakovlev, and K.P. Levenfish, *Astron. Astrophys.* **297**, 717 (1995).
 - [62] D.L. Kaplan, D.A. Frail, B.M. Gaensler, E.V. Gotthelf, S.R. Kulkarni, P.O. Slane, and A. Nechita, *Astrophys. J. Suppl.* **153**, 269–315 (2004) arXiv:astro-ph/0403313.
 - [63] D.G. Yakovlev, A.D. Kaminker, and K.P. Levenfish, *Astron. Astrophys.* **343**, 650–660 (1999) arXiv:astro-ph/9812366.
 - [64] D. Page, M.V. Beznogov, I. Garibay, J.M. Lattimer, M. Prakash, and H.T. Janka, *Astrophys. J.* **898**, 125 (2020) arXiv:2004.06078.
 - [65] A. Dohi, E. Greco, S. Nagataki, M. Ono, M. Miceli, S. Orlando, and B. Olmi, *Astrophys. J.* **949**, 97 (2023) arXiv:2304.08418.
 - [66] N. Iwamoto, *Phys. Rev. Lett.* **44**, 1637–1640 (1980).
 - [67] N. Iwamoto, *Annals of Physics* **141**, 1–49 (1982).
 - [68] P. Jaikumar, M. Prakash, and T. Schäfer, *Phys. Rev. D* **66**, 063003 (2002) arXiv:astro-ph/0203088.
 - [69] S. Reddy, M. Sadzikowski, and M. Tachibana, *Nucl. Phys. A* **714**, 337–351 (2003) arXiv:nucl-th/0203011.
 - [70] A.D. Kaminker, and P. Haensel, *Acta Physica Polonica B* **30**, 1125–1148 (1999) arXiv:astro-ph/9908249.
 - [71] S. Tsuruta, *Phys. Rep.* **292**, 1–130 (1998).
 - [72] W.C.G. Ho, K.G. Elshamouty, C.O. Heinke, and A.Y. Potekhin, *Phys. Rev. C* **91**, 015806 (2015) arXiv:1412.7759.
 - [73] K.S. Thorne, *Astrophys. J.* **212**, 825–831 (1977).
 - [74] A.Y. Potekhin, and G. Chabrier, *Astron. Astrophys.* **609**, A74 (2018) arXiv:1711.07662.
 - [75] M.Y. Fujimoto, T. Hanawa, J. Iben, , I. and M.B. Richardson, *Astrophys. J.* **278**, 813–824 (1984).
 - [76] A. Ritter, Q.A. Parker, F. Lykou, A.A. Zijlstra, M.A. Guerrero, and P. Le Dû, *Astrophys. J. Lett.* **918**, L33 (2021) arXiv:2105.12384.
 - [77] A. Marino, C. Dehman, K. Kovlakas, N. Rea, J.A. Pons, and D. Viganò, arXiv e-prints page arXiv:2404.05371 (2024) arXiv:2404.05371.
 - [78] R. Kothes, *Astron. Astrophys.* **560**, A18 (2013) arXiv:1307.8384.
 - [79] G.E. Allen, K. Chow, T. DeLaney, M.D. Filipović, J.C. Houck, T.G. Pannuti, and M.D. Stage, *Astrophys. J.* **798**, 82 (2015) arXiv:1410.7435.
 - [80] F. Camilloni, W. Becker, P. Predehl, K. Dennerl, M. Freyberg, M.G.F. Mayer, and M. Sasaki, *Astron. Astrophys.* **673**, A45 (2023) arXiv:2303.12686.
 - [81] D. Page, J.M. Lattimer, M. Prakash, and A.W. Steiner, *Astrophys. J. Suppl.* **155**, 623–650 (2004) arXiv:astro-ph/0403657.
 - [82] Y. Lim, C.H. Hyun, and C.H. Lee, *Int. J. Mod. Phys. E* **26**, 1750015–328 (2017).
 - [83] P.S. Shternin, D.D. Ofengeim, C.O. Heinke, and W.C.G. Ho, *Mon. Not. Roy. Astron. Soc.* **518**, 2775–2793 (2023) arXiv:2211.02526.
 - [84] J.M. Lattimer, and M. Prakash, *Astrophys. J.* **550**, 426–442 (2001) arXiv:astro-ph/0002232.